



3-5-13

RESPONSE PROPERTY OF ALLUVIAL VALLEY TO INCIDENT WAVES

Tong JIANG¹ and Eiichi KURIBAYASHI¹

¹Department of Civil Engineering/Regional Planning,
Toyohashi University of Technology, Toyohashi, Aichi, Japan

SUMMARY

In this paper the boundary element method(BEM) is used for the response analyses of axisymmetric valleys subjected to incident waves. The resonance frequency of three-dimensional valley is shown to depend only on two parameters: the one-dimensional resonance frequency at the valley center and the shape ratio, regardless of the incident wave field and impedance contrast. The fundamental resonance amplitude depends on the shape ratio and the impedance contrast. The proposed empirical formulas for estimating the fundamental resonance frequency and the maximum fundamental resonance amplitude at the valley center are verified by numerical examples for valleys with different shape and extensive impedance contrast.

INTRODUCTION

The effect of surface irregularities, such as valley, canyon, dam and hill, on the seismic ground motion has become of major interest lately.

The observations on the seismic response of sediment-filled valleys were made by Tucker and King (1984), and King and Tucker (1984). The results of their instrumental observations for three two-dimensional valleys in the Garm area (Tadjikistan, USSR) had shown that these valleys exhibited specific resonance patterns, the resonance frequency was the same at each site within the valley, regardless of local sediment thicknesses, and the corresponding amplification was the largest in the valley center and decayed toward the edges, where it vanished.

Since the surface motion of semi-cylindrical and semi-elliptical alluvial valley for incident SH waves has been studied by Trifunac (1971), and Wong and Trifunac (1974), the indirect boundary integral equation approach has been used for studying the scattering of SH, P, SV and Rayleigh waves by two-dimensional dipping layers (Wong, 1982; Dravinski, 1983; Dravinski and Mossessian, 1987), and by three-dimensional irregularities (Sanchez-Sesma, 1983). Recently, Bard and Bouchon (1985) have studied the two-dimensional resonance of sediment-filled valleys by using the Aki-Larner technique (1970).

In this paper the BEM based on the direct boundary integral equation is used to analyse the three-dimensional resonance of axisymmetric alluvial valley embedded into a harder half-space subjected to incoming waves, in the cases of body waves (P, SV and SH) and Rayleigh surface wave. The characteristics of the specific resonance patterns for the valleys are investigated.

ANALYTICAL MODEL

The description, formulation and solution of BEM can be referred to

reference (5) for details.

The interface shape of the valley to be analyzed is given by the equation,

$$z = -h \cos\left(\frac{\pi\sqrt{x^2 + y^2}}{2w}\right) \quad (1)$$

where h = maximum depth of the valley, w = maximum horizontal dimension of the valley. The shear wave speed, mass density and Poisson ratio for half-space and valley are c_{s2} and c_{s1} , ρ_2 and ρ_1 , and ν_2 and ν_1 respectively, as shown in Fig.1.

The numerical studies have been performed for four models: model A, B-1, C, and D, having different shape ratio h/w and the same impedance contrast $I_s = \rho_2 c_{s2} / \rho_1 c_{s1}$. The numerical studies were also performed for three models: model B-1, B-2 and B-3, each having the same shape ratio but different impedance contrast. The parameters of these models are shown in table 1. The Poisson ratio are $\nu_1 = 0.3$ and $\nu_2 = 0.25$ for all analytical models.

Table 1 Parameters of Analytical Model

h/w	model A	model B			model C	model D
	0.2	0.4			0.6	0.8
c_{s2}/c_{s1}	4.0	B-1	B-2	B-3	4.0	4.0
ρ_2/ρ_1	1.4	4.0	3.0	2.0	4.0	4.0
I_s	5.6	1.4	1.4	1.25	1.4	1.4
		5.6	4.2	2.5	5.6	5.6

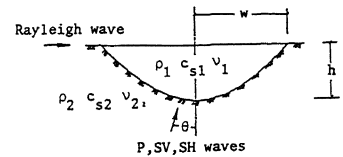


Fig.1 Analytical Model

The spectral displacement amplitude of several point located at surface of the valleys is obtained for each model. The incoming waves are vertically and obliquely incident body waves: P, SV and SH, and Rayleigh surface wave.

RESONANCE MODE

The spectral displacement amplitude at the valley center for the four models subjected to vertical P and S waves is shown in Fig.2. In Fig.2 the ordinate expresses the vertical amplitude (to P wave) and the horizontal amplitude (to S wave), and the abscissa expresses the ratio of frequency f to one-dimensional resonance frequency $f_h^S = c_{s1}/4h$ or $f_h^P = c_{p1}/4h$.

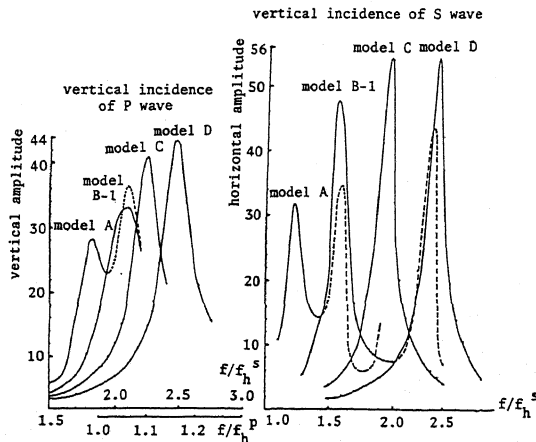


Fig.2 Spectral Displacement Amplitude for Vertically Incident P and S Waves

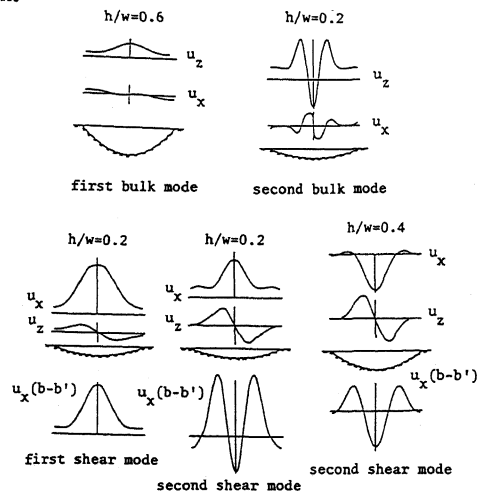


Fig.3 Vertical and Horizontal Resonance patterns of Three-dimensional Valley

The resonance modes can be illustrated by plotting the real parts of the amplitudes, according to the peaks of the spectral displacement along

the valley surface. Fig.3 shows the vertical and horizontal resonance patterns of the valleys for vertical P and S waves.

The figures show the existence in three-dimensional sediment filled valleys of specific resonance patterns, which may be classified in two categories: the S wave resonance is a shearing pattern and may be considered as shear mode, and the P wave resonance is a succession of expansions and contractions, and may be considered as bulk mode. For each model, the vertical and horizontal amplitudes are coupled. The maximum horizontal motion for bulk modes, and the maximum vertical motion for shear modes are displayed at the mid-edges. For the fundamental bulk and shear modes, the amplitude is the largest at the valley center and decays toward the edges.

The spectral displacement amplitude of five surface sites, regularly spaced from the center to the edge, for each model is displayed in Fig.4. The figures show that the fundamental resonance frequency is the same at each site.

It is very clear that, when the shape ratio of the valley becomes larger, the ratio of fundamental resonance frequency to one-dimensional resonance frequency and the resonance amplitude at the valley center become larger.

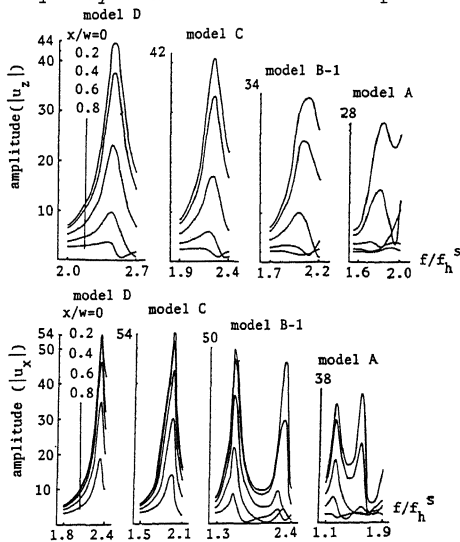


Fig.4 Spectral Displacement Amplitude of Five Surface Sites for Vertically Incident P and S Waves

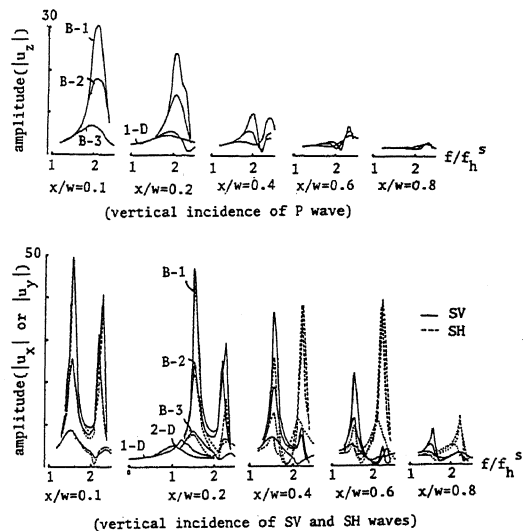


Fig.5 Effect of Impedance Contrast

SENSITIVITY STUDY

Effect of impedance contrast The parameter study is made for model B-1, B-2 and B-3, each having the same shape ratio $h/w = 0.4$ and different impedance contrast from 2.5 to 5.6. The effect of impedance contrast is illustrated in Fig.5 for vertical P and S waves.

The main result is that the peaks of the spectral displacement amplitude occur at about the same frequencies (scaled to f_h^S), regardless of the impedance contrast. Besides, for $I_s = 2.5$ (model B-3) the spectral displacement amplitude of one-dimensional model (a horizontal layer), denoted as 1-D, and two-dimensional model, denoted as 2-D, are illustrated also. It is very clear, when the soft deposit is restricted more strongly by the half-space, the fundamental resonance frequency becomes higher and resonance amplitude becomes larger.

As expected, the amplification values increase with the increase of impedance contrast.

Effect of obliquely incident body waves Here we will show some features for

model D. In Fig.6 the spectral displacement amplitude is given for surface sites of left and right sides of the valley. The incident waves are P and SV.

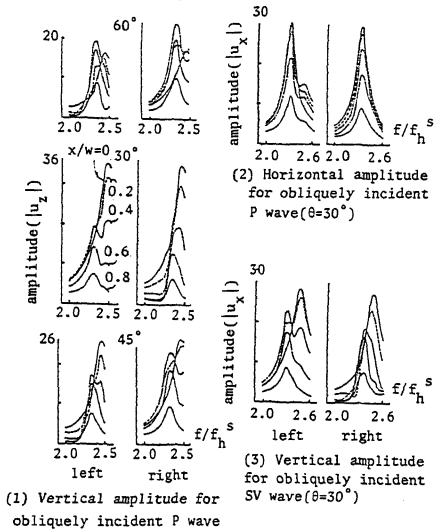


Fig.6 Spectral Displacement Amplitude of Left and Right Sites for Obliquely Incident P and SV Waves

Fig.6 (1) plots the spectral vertical displacement amplitude of several sites for left and right sides to obliquely incident P waves with three incident angles: 30°, 45° and 60°. Because the obliquely incident P wave has both the vertical and horizontal components, The bulk and shear resonance modes will be excited. Corresponding to the shear resonance frequency the mid-edges display peaks and corresponding to the bulk resonance frequency the valley center displays a peak. Moreover the figure shows that the amplification values at the center depend on the value of the vertical component of the free field for obliquely incident P waves.

Fig.6 (2) and (3) plot the spectral horizontal displacement amplitude to obliquely incident P and SV waves ($\theta = 30^\circ$). They also show that the resonance frequencies of each mode, either bulk or shear, are not affected by obliquely incident body waves.

Effect of incident Rayleigh wave In Fig.7 the spectral displacement amplitude is given for the left and right sides of the model C and D. The figure shows that the resonance frequencies of each mode, either bulk or shear, are not affected by incident surface wave. In table 2 the column of the free field means the ratio of the component of Rayleigh wave to the component of vertically incident body wave, and the others mean the resonance amplitude ratios at the valley center of the incident Rayleigh wave to the vertically incident body wave. The ratios are nearly equal for vertical amplitudes. However, for horizontal amplitudes the ratios decrease with the increase of the model's depth. Because the horizontal displacement of Rayleigh wave decreases versus the depth faster than the vertical one does, the decrease of the ratios of horizontal resonance amplitude with respect to the increase of the model's depth can be interpreted by the decrease of the input exciting level for the horizontal direction.

Table 2 Ratio of the Resonance Amplitudes of Rayleigh Wave and Vertically Incident Body Wave

items	model A	model C	model D	free field
ratio of vertical amplitude	0.83	0.75	0.77	0.78
ratio of horizontal amplitude	0.44	0.22	0.16	0.50

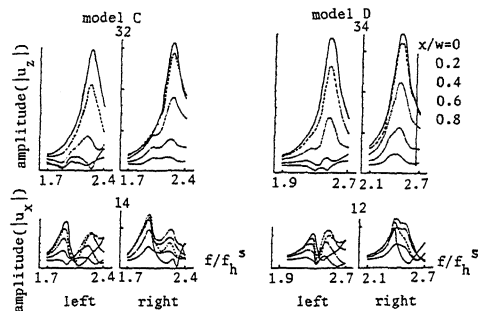


Fig.7 Spectral Displacement Amplitude of Left and Right Sites for Incident Rayleigh Wave

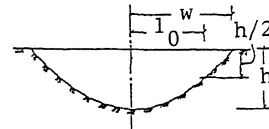


Fig.8 Equivalent Width

RESONANCE FREQUENCY AND AMPLITUDE

From the sensitivity studies the numerical results show that the resonance frequency depends only on two parameters, namely, the one-dimensional resonance frequency at the valley center and the shape ratio. To apply the results from cosine-shaped valley to any axisymmetric valley shape, we will introduce an equivalent shape ratio h/l_0 , where l_0 is the half width over which the sediment thickness is more than half its maximum value (Fig.8).

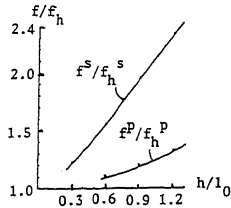


Fig.9 Dependence of Dimensionless Resonance Frequency on Shape Ratio

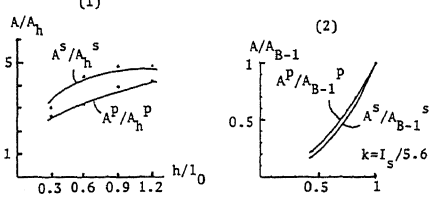


Fig.10 Dependence of Dimensionless Resonance Amplitude on Shape Ratio and Impedance Contrast

From the results displayed in Fig.9, we may obtain the approximate empirical formulas for the fundamental resonance frequencies,

$$f^S/f_h^S = \sqrt{[1 + 3.3 (h/l_0)^{1.6}]} \tag{2}$$

$$f^P/f_h^P = \sqrt{[1 + 0.5 (h/l_0)^2]} \tag{3}$$

where f^S and f_h^S , and f^P and f_h^P are the three- and one-dimensional fundamental shear and bulk resonance frequencies, respectively.

The numerical results also show that the resonance amplitudes at the valley center for vertically incident P and S waves are to depend on the one-dimensional resonance amplitudes, the shape ratio, and the impedance contrast.

From the results displayed in Fig.10 (1) expressed the effect of shape ratio and Fig.10 (2) expressed the effect of impedance contrast for model B, we have obtained the fundamental resonance amplitudes A^S and A^P at the valley center,

$$A^S = 2 (1 + 3.56 \sqrt[4]{h/l_0})(0.21I_s^2 - 0.18I_s) \tag{4}$$

$$A^P = 2 (1 + 2.87 \sqrt{h/l_0})(0.17I_p^2 + 0.10I_p) \tag{5}$$

where, $I_p = c_{p2} \rho_2 / c_{p1} \rho_1$.

To investigate how eq. (2),(3) and eq. (4),(5) are applicable to axisymmetric valley with different shape and parameter, three models have been analyzed. The models and parameters are shown in Fig.11 and table 3.

Table 3 Parameters of Three Models

parameter	model 1	model 2	model 3
h/l_0	1.0	0.67	0.5
v_1	0.3	0.35	0.4
v_2	0.2	0.29	0.3
c_{s2}/c_{s1}	2.0	2.5	3.5
ρ_2/ρ_1	1.3	1.25	1.4
I_s	2.6	3.13	4.9

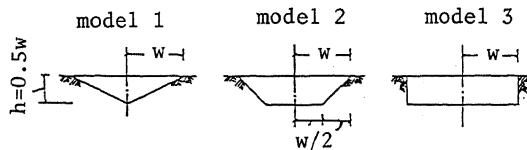


Fig.11 Analytical Models for Checking the Empirical Formulas

The results from eq. (2),(3) and eq. (4),(5), and from the spectral displacement amplitude obtained by calculation, are shown in table 4. In the table the bracketed values mean the relative errors of the proposed formulas.

The results of table 4 show that the proposed approximate empirical formulas for estimating the fundamental resonance frequency and the fundamental resonance amplitude at the valley center predict very accurately the fundamental resonance properties for valleys with different shapes and extensive impedance contrasts.

Table 4 Comparison of Proposed Formulas with Calculation

items		model 1	model 2	model 3
fundamental bulk	by eq.(3)	2.29(2.6%)	2.31(3.8%)	2.60(4.0%)
resonance frequency	by calculation	2.35	2.40	2.50
fundamental shear	by eq.(2)	2.07(6.2%)	1.65(5.1%)	1.45(0.0%)
resonance frequency	by calculation	1.95	1.57	1.45
fundamental bulk	by eq.(5)	8.53(7.8%)	10.50(0.5%)	16.70(1.2%)
resonance amplitude	by calculation	7.91	10.55	16.91
fundamental shear	by eq.(4)	8.67(2.7%)	12.61(17.4%)	33.22(14.7%)
resonance amplitude	by calculation	8.91	15.26	38.94

CONCLUSIONS

The three-dimensional resonance of axisymmetric valley has been clarified by using boundary integral equation approach.

The fundamental resonance frequencies depend only on two parameters, namely, the one-dimensional resonance frequency at the valley center and the shape ratio, regardless of the incident wave field and the impedance contrast. The fundamental resonance amplitudes at the valley center depend on the shape ratio and the impedance contrast. The proposed empirical formulas can estimate approximately the fundamental resonance frequencies and amplitudes.

We hope these results may find practical applications in earthquake engineering and seismic microzonation studies.

ACKNOWLEDGEMENTS

The authors are indebted to Dr. H. Tajimi, honorary professor of Nihon University, for his helpful suggestions.

REFERENCES

1. Aki, K. and Larner, K. L., "Surface Motion of a Layered Medium Having an Irregular Interface due to Incident SH Waves," *J. Geophys. Res.*, 75, 933-951, (1970).
2. Bard, P. Y. and Bouchon, M., "The Two-dimensional Resonance of Sediment-filled Valley," *Bull. Seism. Soc. Am.*, 75, 519-541, (1985).
3. Dravinski, M., "Scattering of Plane Harmonic SH Waves by Dipping Layers of Arbitrary Shape," *Bull. Seism. Soc. Am.*, 73, 1303-1319, (1983).
4. Dravinski, M. and Mossessian, T. K., "Scattering of Plane Harmonic P, SV and Rayleigh Waves by Dipping Layers of Arbitrary Shape," *Bull. Seism. Soc. Am.*, 77, 212-235, (1987).
5. Jiang, T. and Kuribayashi, I., "The Three-dimensional Resonance of Axisymmetric Sediment Filled Valleys," *Soils and Foundations* (to be published).
6. King, J. L. and Tucker, B. E., "Observed Variations of Earthquake Motion over a Sediment-filled Valley," *Bull. Seism. Soc. Am.*, 74, 987-998, (1984).
7. Sanchez-Sesma, F. J., "Diffraction of Elastic Waves by Three-dimensional Surface Irregularities," *Bull. Seism. Soc. Am.*, 73, 1621-1636, (1983).
8. Trifunac, M. D., "Surface Motion of a Semi-cylindrical Alluvial Valley for Incident SH Waves," *Bull. Seism. Soc. Am.*, 61, 1755-1770, (1970).
9. Tucker, B. E. and King, J. L., "Dependence of Sediment-filled Valley Response on the Input Amplitude and the Valley Properties," *Bull. Seism. Soc. Am.*, 74, 153-165, (1984).
10. Wong, H. L. and Trifunac, M. D., "Surface Motion of a Semi-elliptical Alluvial Valley for Incident Plane SH Waves," *Bull. Seism. Soc. Am.*, 64, 1389-1418, (1974).
11. Wong, H. L., "Diffraction of P, SV and Rayleigh Waves by Surface Topographies," *Bull. Seism. Soc. Am.*, 72, 1167-1184, (1982).